The Astronomical Journal, 126:37–46, 2003 July

PKS 0736+017: A STRIKING OPTICAL FLARE AND INTRIGUING MICROVARIABILITY

S. D. Clements, A. Jenks, and Y. Torres
Department of Physics and Space Sciences and the SARA Observatory, Florida Institute of Technology, Melbourne, FL 32901;
clements@astro.fit.edu
Received 2002 November 15; accepted 2003 March 18

ABSTRACT

The compact, flat-spectrum radio quasar PKS 0736+017 was monitored for microvariability on 10 nights in early 2002 using the 0.9 m SARA telescope on Kitt Peak in Arizona. On January 14, PKS 0736+017 flared dramatically, brightening by 1.3 *R* mag in 2 hours. Prior to the flare, PKS 0736+017 exhibited quasi-periodic variations. During and after the flare, more complex oscillations occurred. Impressive variability was displayed on two additional nights in January, while observations during the following 3 months found PKS 0736+017 to be fairly quiescent. PKS 0736+017 was somewhat redder while brighter and fading than when dimmer but flaring. During flaring or fading episodes, the color remained approximately constant. Thus, it appears that for these observations, color is related more to the nature of the variation than it is to the brightness level.

Key words: quasars: general — quasars: individual (PKS 0736+017)

On-line material: machine-readable table

1. INTRODUCTION

PKS 0736+017 is a flat-spectrum radio source with a compact core (Gower & Hutchings 1984; Romney et al. 1984) and a one-sided parsec-scale jet (Bloom et al. 1999; Kellermann et al. 1998). This high-polarization quasar (Véron-Cetty & Véron 2001) with a redshift of $z = 0.191$ (Tadhunter et al. 1993; Lynds 1967) has been shown to reside in an elliptical host galaxy (Falomo & Ulrich 2000; McLure et al. 1999; Wright, McHardy, & Abraham 1998). The spectral energy distribution of PKS 0736+017 extends from the radio through the X-ray (Fossati et al. 1998; Impey & Neugebauer 1988). In its long-term optical light curve, PKS 0736+107 is seen to exhibit several unresolved short-term flares superposed on a slowly varying baseline (Pica et al. 1988; Clements et al. 1995). Both the long-term variations and the short-term flares have amplitudes of approximately 0.7 m_{pg} magnitude. Long-term radio monitoring has resolved numerous flares with timescales of a few months to a few years (Aller et al. 1985; Medd et al. 1973; Andrew et al. 1978; Teräsranta et al. 1998). These long-term monitoring campaigns were not designed to detect intraday variability.

Intraday variability or microvariability is defined by Miller, Carini, & Goodrich (1989) as "significant variations that occur on timescales less than a day." Such short-term variations in sources have been reported across the electromagnetic spectrum from the radio through the γ-ray (Wiita 1993; Wagner & Witzel 1995). For this work, the term microvariability refers to variations in the optical regime. Microvariability was reported as early as 1963 (Matthews & Sandage 1963) for 3C 48 using photographic photometry. Photoelectric photometry was used by Racine (1970) to detect microvariability in BL Lac. However, it was only after CCD technology became prevalent along with the use of CCDs as multistar photometers that many observers began looking for microvariability in active galactic nuclei (AGNs).

Numerous models have been put forth to explain microvariability in AGNs. Among these models are interstellar scintillation, microlensing by stars in the host galaxy, turbulence in relativistic jets, directional fluctuations of relativistic jets, and accretion disk instabilities. (See Wiita 1993 and Wagner & Witzer 1995 for nice reviews of many of these models.) Studies have shown that microvariability is more prevalent among radio-loud sources than among radio-quiet sources (Jang & Miller 1995, 1997; Gopal-Krishna, Sagar, & Wiita 1993; Sagar, Gopal-Krishna, & Wiita 1996). This dichotomy supports jet models, since radio-quiet quasars are thought to lack jets (Antonucci, Barvainis, & Alloin 1990) or to have only very weak jets (Miller, Rawlings, & Saunders 1993; Kellermann et al. 1994). The detection of microvariability in some radio-quiet objects suggests that disk models may be viable for these sources. Indeed, it is not unthinkable that both disk and jet phenomena may contribute to the microvariability observed in a source.

2. OBSERVATIONS

PKS 0736+017 was observed on 10 nights from 2002 January to April using the Southeastern Association for Research in Astronomy (SARA) 0.9 m telescope at Kitt Peak Astronomical Observatory in Arizona. Images were made with an Apogee AP7 CCD camera at the f/7.5 Cassegrain focus. The CCD chip has dimensions 512 × 512 pixels with each pixel being 24 μm on a side. At $0\farcs73$ pixel^{-1}, the CCD chip images $6\farcm3 \times 6\farcm3$ of the sky. Most nights images were made with 2 × 2 binning (to improve sensitivity and thus reduce exposure times) resulting in an effective CCD chip dimension of 256 × 256 pixels, or $1\farcs5$ pixel dimension. On January 14 and 15, exposures were made through an *R* filter. For the remaining nights, exposures were made alternately through *R* and *V* filters. Details of the observations are given in Table 1, which lists the date, the number of observations through the *V* and *R* filters, the typical exposure time, and the binning used for the CCD observations.

Images were calibrated in the usual way to remove the effects of bias, thermal noise, and nonuniform pixel sensitivity. Magnitudes were then obtained for the quasar and several check stars in the field of the quasar using the

TABLE 1
SUMMARY OF OBSERVATIONS

Night	Number V	Number R	Exposure[a] (s)	Binning
2002 Jan 14	...	390	60	2 × 2
2002 Jan 15	...	25	360	1 × 1
2002 Jan 21	75	75	120	1 × 1
2002 Jan 23	40	40	120	1 × 1
2002 Feb 20.....	26	29	120	1 × 1
2002 Mar 16.....	40	40	90	2 × 2
2002 Mar 18.....	50	50	60	2 × 2
2002 Mar 22.....	10	16	90	2 × 2
2002 Apr 22.....	17	22	90	2 × 2
2002 Apr 23.....	3	3	90	2 × 2

[a] Typical exposure time for the night.

aperture photometry tool in the MIRA AP[1] software. Star 2 from the comparison star sequence in Smith et al. (1985) was used as the reference magnitude for the aperture photometry. Table 2 summarizes the V observations for PKS 0736+017 and the check stars. The R observations are summarized in Table 3. In these tables the date and number of exposures for the night are listed in columns (1) and (2), respectively. The mean magnitude, standard deviation in the magnitude, and the minimum and maximum magnitudes for the night are listed in columns (3)–(6) for PKS 0736+017. In the remaining columns the mean magnitude and the standard deviations in the magnitudes of the check stars are listed. Table 4 lists the Julian Date and the V and R magnitudes for PKS 0736+017 and each check star. The scatter in the check star magnitudes is larger than the formal errors, thus the scatter in the check star magnitudes is a more conservative estimate of the uncertainty in the magnitudes of PKS 0736+017. Note that when PKS 0736+017 is bright, the uncertainty in its magnitude is comparable to the scatter in the magnitude of the brighter check stars and when it is fainter, the uncertainty is comparable to that of the scatter in the fainter check stars.

[1] MIRA is a registered trademark and MIRA AP is a trademark of Axiom Research, Inc.

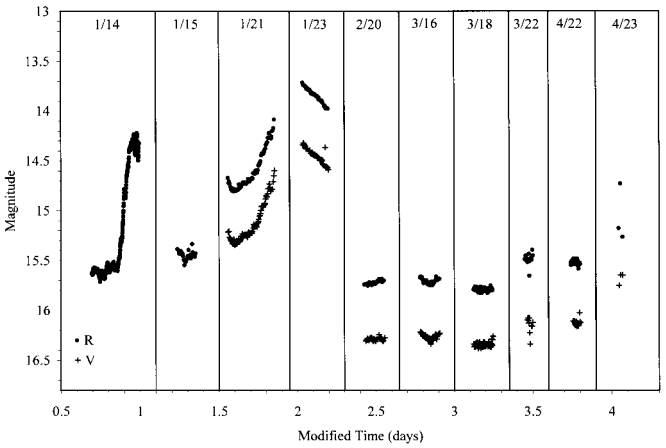

FIG. 1.—Light curve for PKS 0736+017. Ten nights of observations are shown. Dates are listed at the top of each panel. Times are modified for display purposes to allow variations within each night to be seen. On January 14 and 15 only R observations were made. On the remaining nights both V and R observations were made. The R observations are brighter than the V observations in each panel.

3. ANALYSIS

A light curve including observations on all nights is shown in Figure 1. In this figure times are in units of days and were modified for display purposes to allow variations within each night to be seen. Observation dates are shown near the top of the figure. Figure 2 shows similar light curves for the check stars in the field with their magnitudes modified for display purposes. In Figure 1, PKS 0736+017 is seen to vary between $R = 15.8$ and 13.7. Microvariability was not evident on three of the nights (January 15, March 22, and April 23) when poor conditions resulted in large scatter in the check stars' magnitudes. The slow brightening in R seen on February 20 is mimicked in the comparison stars and is thus not real. Low-amplitude variability was detected on March 16. On three nights the microvariability had an amplitude greater than 0.2 mag. Though PKS 0736+017 increased in brightness by more than 0.5 mag on both January 14 and January 21, the variability behavior on the two nights is quite different. On January 14, PKS 0736+017 brightened by 1.3 R mag in just over 2 hr—a rate of 0.6 mag hr^{-1}. On January 21 it bright-

TABLE 2
SUMMARY OF OBSERVATIONS: V FILTER

		PKS 0736+017				C2		C3		C4	
NIGHT	N	V_{ave}	σ_V	V_{min}	V_{max}	V_{ave}	σ_V	V_{ave}	σ_V	V_{ave}	σ_V
2002 Jan 21	75	15.127	0.198	14.596	15.344	14.937	0.009	15.627	0.017	16.196	0.016
2002 Jan 23	40	14.446	0.071	14.322	14.588	14.908	0.016	15.625	0.087	16.217	0.019
2002 Feb 20.....	26	16.289	0.015	16.243	16.312	14.920	0.012	15.628	0.016	16.194	0.015
2002 Mar 16.....	40	16.266	0.027	16.214	16.336	14.921	0.015	15.629	0.010	16.211	0.014
2002 Mar 18.....	50	16.342	0.023	16.259	16.381	14.926	0.015	15.641	0.014	16.211	0.019
2002 Mar 22.....	10	16.148	0.080	16.076	16.337	14.948	0.048	15.651	0.049	16.241	0.074
2002 Apr 22.....	17	16.124	0.031	16.024	16.158	14.939	0.032	15.642	0.027	16.217	0.051
2002 Apr 23.....	3	15.681	0.060	15.646	15.751	14.788	0.106	15.500	0.193	16.220	0.277
All[a]	262	15.652	0.730	14.322	16.381	14.925	0.027	15.630	0.045	16.208	0.036
Good[b].....	249	15.631	0.742	14.322	16.381	14.926	0.018	15.631	0.038	16.206	0.023

[a] Results for the entire data set.
[b] Results for the entire data set excluding data from March 22 and April 23.

TABLE 3
SUMMARY OF OBSERVATIONS: *R* FILTER

		PKS 0736+017				C2		C3		C4	
NIGHT (1)	*N* (2)	R_{ave} (3)	σ_R (4)	R_{min} (5)	R_{max} (6)	R_{ave} (7)	σ_R (8)	R_{ave} (9)	σ_R (10)	R_{ave} (11)	σ_R (12)
2002 Jan 14	390	15.198	0.530	14.220	15.713	14.499	0.017	14.707	0.018	15.758	0.019
2002 Jan 15	25	15.445	0.045	15.335	15.547	14.488	0.043	14.719	0.070	15.778	0.041
2002 Jan 21	75	14.602	0.192	14.086	14.805	14.504	0.007	14.681	0.016	15.728	0.012
2002 Jan 23	40	13.847	0.076	13.717	13.978	14.488	0.022	14.696	0.009	15.753	0.015
2002 Feb 20	29	15.724	0.019	15.683	15.753	14.490	0.023	14.676	0.010	15.727	0.012
2002 Mar 16	40	15.707	0.024	15.659	15.748	14.488	0.008	14.679	0.009	15.744	0.015
2002 Mar 18	50	15.791	0.017	15.752	15.827	14.498	0.015	14.695	0.014	15.750	0.014
2002 Mar 22	16	15.489	0.055	15.394	15.654	14.485	0.043	14.681	0.031	15.687	0.121
2002 Apr 22	22	15.524	0.024	15.482	15.583	14.500	0.020	14.687	0.022	15.741	0.040
2002 Apr 23	3	15.056	0.288	14.727	15.265	14.507	0.106	14.652	0.195	15.388	0.389
All[a]	690	15.175	0.061	13.717	15.827	14.497	0.020	14.699	0.027	15.748	0.044
Good[b]	671	15.168	0.061	13.717	15.827	14.498	0.016	14.698	0.020	15.750	0.021

[a] Results for the entire data set.
[b] Results for the entire data set excluding data from January 15, March 22, and April 23.

ened dramatically as well (0.7 mag), but over a much longer time (6 hr) for a rate of 0.1 mag hr^{-1}. It faded at a slower rate still on January 23, dimming by 0.26 *R* mag in 3.9 hr for a rate of 0.07 mag hr^{-1}.

To ensure that the smaller amplitude variations seen throughout the light curve are not the result of seeing-induced variations, as described by Cellone, Romero, & Combi (2000), the check star's PSF was examined. Variations in the FWHM of the PSF were found to be unrelated to the variations of PKS 0736+017 or the check stars; thus, the low-amplitude variations seen in PKS 0736+017 are real.

3.1. *January 14*

The dramatic brightening on January 14 warrants a closer look. Figure 3 shows the PKS 0736+017 data for January 14 only. The check stars' light curves for January 14 are shown in Figure 4. Visual inspection indicates that PKS 0736+017 exhibited continuous low-amplitude variability (0.1 mag) while in its low state with a variability timescale of 45 minutes. It continued to exhibit small-scale variability during the major outburst portion of the light curve. Once in its high state unusual oscillatory behavior becomes apparent, with higher variability amplitude (0.2 mag) and shorter timescale (30 minutes).

A yet closer look at the oscillatory behavior of PKS 0736+017 during its high state is shown in Figure 5. Note that the oscillations grow in timescale (time between local minima or maxima) and in amplitude (local maximum to local minimum variation) for the rest of the night's observations. Despite this growth in amplitude the local maxima of the oscillations approach a constant value so that it is the depths of the local minima that increase with each oscillation. Similar behavior, but with longer oscillation timescales, was observed by Pollock (1999) for the BL Lac object ON 231 during the declining phase of a major outburst in 1998.

Due to the intriguing appearance of the observed variations, a search was made for periodic or quasi-periodic components using two methods, the Scargle periodogram (Scargle 1982) as described in Horne & Baliunas (1986) and the CLEAN algorithm of Roberts, Lehár, & Dreher (1987). Time series analysis with these techniques can be used to detect periodic variations in unevenly sampled data. The CLEAN algorithm was originally developed for use in aperture synthesis (Hogbom 1974). Roberts et al. (1987) describe its application to spectral analysis, indicating that it is especially suited for use when a small number of components at discrete frequencies dominate the time series data. The classical periodogram makes use of the discrete Fourier transform which is defined for unevenly sampled data (Deeming 1975). Scargle modified the classical periodogram to improve the statistical behavior. The Scargle periodogram is equivalent to least-squares fitting of sinusoids to the data. Horne & Baliunas (1986) provide a "prescription" for detecting and evaluating the significance of periodic signals in unevenly sampled time series data using the Scargle periodogram. Wilkat et al. (2002) used these techniques to

TABLE 4
JULIAN DATES AND *V* AND *R* MAGNITUDES FOR PKS 0736+017 AND CHECK STARS

Julian Date	Object Magnitude	C2 Magnitude	C3 Magnitude	C4 Magnitude	Filter
2,452,295.65861	15.215	14.944	15.630	16.193	*R*
2,452,295.66284	15.207	14.936	15.618	16.197	*R*
2,452,295.66685	15.269	14.951	15.636	16.219	*R*
2,452,295.67076	15.275	14.953	15.637	16.186	*R*
2,452,295.67490	15.294	14.951	15.641	16.186	*R*

NOTE.—Table 4 is presented in its entirety in the electronic edition of the *Astronomical Journal*. A portion is shown here for guidance regarding its form and content.

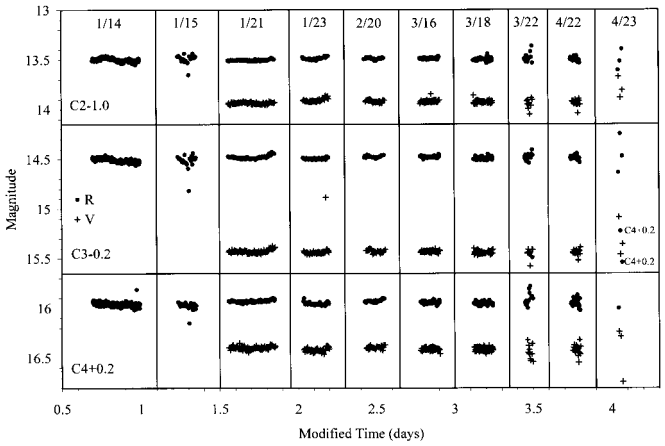

FIG. 2.—Light curve for the check stars. Ten nights of observations are shown for all three check stars with the same modified time axis as in Fig. 1. Dates are listed at the top of each panel. Here the magnitudes of the check stars have also been modified for display purposes. Prior to plotting, 1.0 mag was subtracted from both the *V* and *R* data for check star 2. Similarly, 0.2 mag was subtracted from the *V* and *R* data for check star 3, and 0.2 mag was added to the *V* and *R* data for check star 4. Note that two *R* data points for C4 are in the C3 panel and are labeled "C4+0.2." As in Fig. 1, the *R* observations for each check star are brighter than the *V* observations. Finally, note that the magnitude range shown is the same as in Fig. 1.

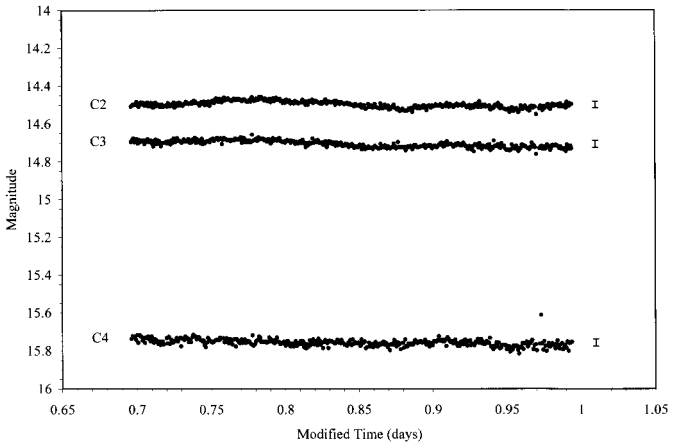

FIG. 4.—January 14 light curve for the check stars. The three data points with error bars show the mean magnitudes and the standard deviations in the magnitudes of the check stars.

investigate the longer timescale variations in the January 14 PKS 0736+017 data.

It is the high-frequency variations that are of interest here. Thus, the low-frequency variations (including the dramatic flare) were removed from the light curve. This was accomplished via two different methods: removal of a boxcar average and removal of linear fits to segments of the light curve. With the boxcar method, the average of the flux within a bin of 30 successive data points (approximately 33 minutes) was computed. This was then removed from the light curve, thus largely (but not entirely) eliminating low-frequency components. To further eliminate low-frequency components, a linear fit to the resulting data was also removed, leaving a light curve whose linear fit has a slope of zero. The residuals that result from removing the boxcar averaged data from the light curve are shown in Figure 6*a*. The linear-fits method involved fitting lines to segments of the light curve that showed approximately linear trends. These linear trends were removed from each segment and the entire data set was adjusted to remove any overall linear trend. The residuals remaining after these linear fits were removed are shown in Figure 6*b*.

Both the boxcar method and the linear-fits method have positive and negative features. The boxcar method did a better job of removing the longer timescale variations than the linear-fits method. It also did a better job of handling the transition out of the low state. The linear-fits method underestimates the brightness during this transition. Thus, residuals obtained by subtracting the linear fit from the data show an artificial event during the transition. A drawback of the boxcar method is that it reduces the effective duration of the data set by approximately 30 minutes, which is not the case for the linear-fits method. Another drawback of the boxcar method is that the boxcar smoothed data still exhibit oscillations when in the high state. Removal of the boxcar smoothed data actually increases the amplitude of the high-state oscillations in the residuals. Again, this is not the case with the linear-fits method. Thus, the two methods

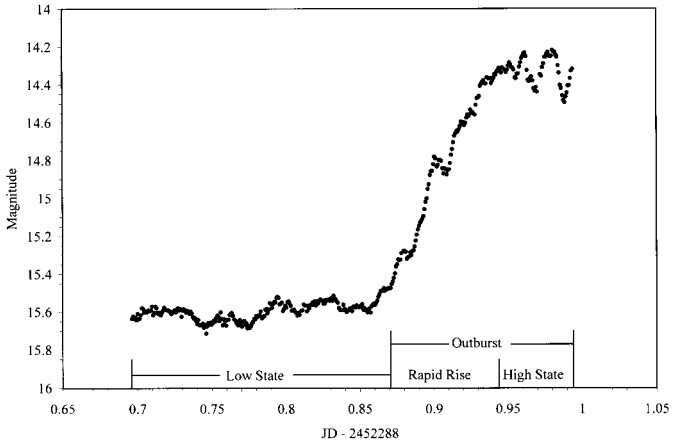

FIG. 3.—January 14 light curve for PKS 0736+017. The low-state, rapid-rise, high-state, and outburst subsets are subject to the time series analysis described in the text. The extent in time for each subset is indicated along the Modified Julian Date axis.

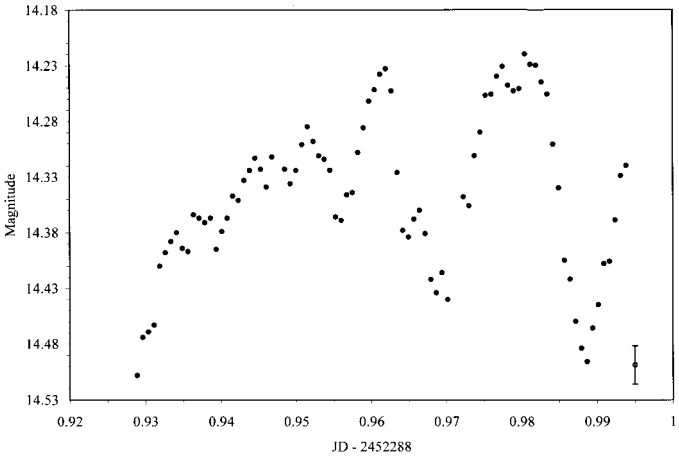

FIG. 5.—High-state oscillations in PKS 0736+017 on January 14. The data point with the error bars shows the mean magnitude and standard deviation in the magnitudes for check star C2. The scatter in the magnitudes of the check star is indicative of the uncertainty in the magnitudes of PKS 0736+017.

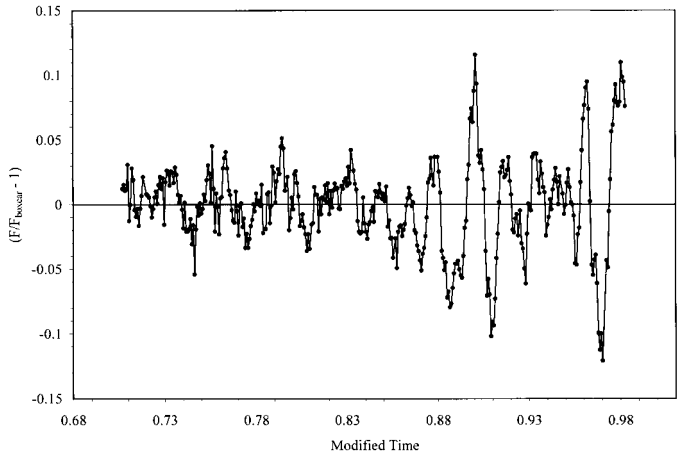

FIG. 6*a*

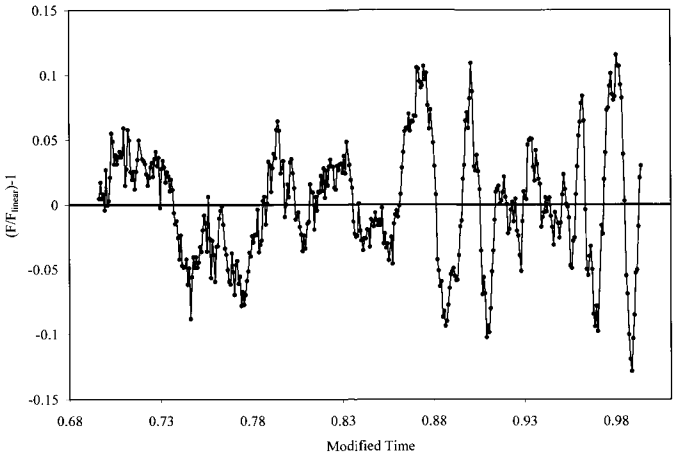

FIG. 6*b*

FIG. 6.—(*a*) Residuals after removal of the boxcar-smoothed data from the PKS 0736+017 data. (*b*) Residuals after removal of linear fits to subsets of the PKS 0736+017 data.

complement each other, with the boxcar method being more appropriate for the low state and the linear-fits method being more appropriate for the rest of the data set.

In Figure 6 the short-term variability behavior changes character at about the onset of the outburst. For this reason the Scargle periodogram and the CLEAN algorithm were applied not only to the full data set of residuals, but also to subsets. These subsets, identified in Figure 3, include the "low state" (modified time < 0.871), the "rapid rise" ($0.871 <$ modified time < 0.944), the "high state" (modified time > 0.944), and the "outburst" (modified time > 0.871). Note that the outburst subset includes both the rapid rise and the high state. In Table 5 the periods for the three strongest signals identified with the time series analysis are listed in order of strength. A signal is listed only if the periodogram analysis indicates that it has a probability greater than 90% that it is not the result of random noise. Of particular note are the results for the low state and the outburst subsets. The CLEAN power spectrum and Scargle periodogram of the low-state subset (Figs. 7*a* and 7*b*) each show a strong peak corresponding to a 45 minute "periodic" variation. The strongest peaks identified in the outburst subset by both the CLEAN and the Scargle periodogram analysis correspond to 29 and 38 minute variations. There are no peaks in the CLEAN spectral window functions of either the low or outburst subsets that would indicate that these signals are spurious effects due to the sampling. The spectral window is the Fourier transform due to the sampling details of a time series.

A comment about the false alarm levels shown in Figure 7*b* is warranted. Analysis of a pure noise source with the Scargle periodogram will produce a peak of that level or higher in a fraction F of cases in which the variance is the same as for the actual data. Scargle (1982) called this quantity F the false alarm probability and derived an analytical expression relating it to the power level. The probability that the data contain a signal is thus $1 - F$. The horizontal lines in Figure 7*b* indicate four of these levels. Consider for example the horizontal line labeled with 1% in Figure 7*b*. In only 1 out of 100 pure noise signals having the same total variance as the true signal would the power level reach or exceed this level. These probability levels were verified using simulated Gaussian noise signals having the same variance as the low-state data and the same time sampling. Indeed, the probability levels shown in Figure 7*b* were found by the simulations to be somewhat conservative, slightly overestimating the false alarm probability.

The results for the linear-fits residuals are similar to those for the boxcar residuals and are tabulated in Table 6. There are additional low-frequency peaks identified for some subsets because the linear-fits method was not as effective as the boxcar method at removing the lower frequency components. For example, a very strong 2.2 hr signal is identified in the low-state subset of residuals from the linear-fits method that is not evident in the residuals from the boxcar method.

Reconstructions of the data using the periods, phases, and amplitudes of the sinusoidal signals detected with the

TABLE 5

SIGNALS IDENTIFIED IN THE PKS 0736+017 BOXCAR RESIDUALS

	SCARGLE PERIODOGRAM RESULTS						CLEAN RESULTS		
SUBSET	T_1 (minutes)	Prob_1 (%)	T_2 (minutes)	Prob_2 (%)	T_3 (minutes)	Prob_3 (%)	T_1 (minutes)	T_2 (minutes)	T_3 (minutes)
Low	44.4	>99.9	23.0	98.8	20.1	90.1	45.0	23.5	19.9
Rise.....	27.6	>99.9	...	...	...	...	27.6	...	...
High.....	25.0	>99.9	42.3	98.1	...	...	24.0	42.2	...
Outburst	29.3	>99.9	38.4	>99.9	22.7	>99.9	29.1	22.2	38.7
All data	29.6	>99.9	39.3	>99.9	23.5	>99.9	29.4	24.0	39.3

NOTE.—Periods of approximately 20 minutes are obtained from analysis of the check stars (see Table 7) and thus should be considered as suspect.

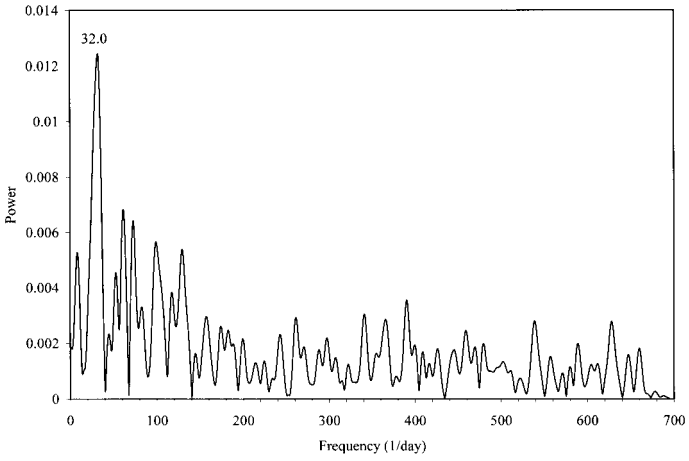

FIG. 7*a*

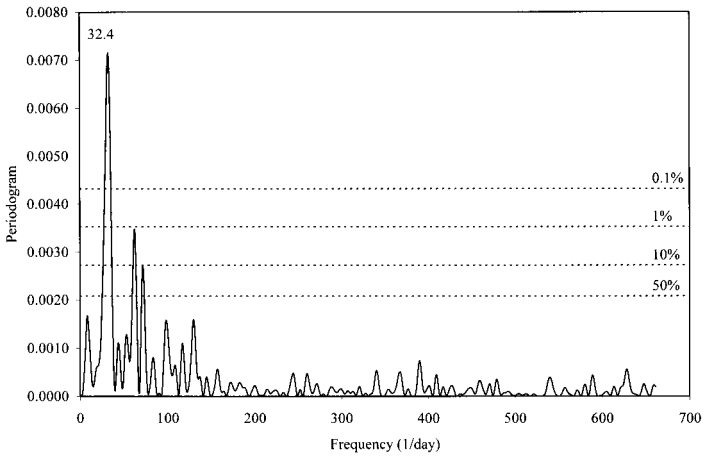

FIG. 7*b*

FIG. 7.—(*a*) Power spectrum obtained using the CLEAN algorithm on the low-state subset of residuals obtained using the boxcar method. The 32 day^{-1} signal corresponds to a sinusoidal signal with a 45.0 minute period. (*b*) Scargle periodogram for the low-state subset of residuals obtained using the linear-fits method. The 32.45 day^{-1} signal corresponds to a sinusoidal signal with a 44.4 minute period. The horizontal lines show the 50%, 10%, 1%, and 0.1% probability levels that the signal arises from a pure noise source. Thus, the probability that the 44.4 minute signal is not due to pure noise is greater than 99.9%.

CLEAN algorithm are shown superposed on the low-state and outburst residuals in Figures 8 and 9, respectively. The Scargle periodogram analysis identified nearly identical frequencies as those used in these figures. (Compare Tables 5 and 6.) The sinusoid with a frequency corresponding to the strongest signal in the low-state subset is shown in Figure 8. Note that this 45.0 minute signal represents five cycles in the low-state subset. The 23 minute peak is likely a harmonic of the 45 minute signal. Scargle periodogram analysis is equivalent to the reduction of the sum of the squared residuals in least-squares fitting of sine waves to the data (Scargle 1982). The power level of the periodogram analysis mirrors the χ^2 merit function (the sum of the squared residuals between the data and the fitted sine wave). That is, the maximum in the periodogram occurs at the same frequency that minimizes the χ^2 merit function (Scargle 1982). The power level in the periodogram of Figure 7*b* is above the 0.1% false alarm level for values between 40 and 50 minutes. Thus, a conservative assessment of the characteristic timescale of the signal in the low-state subset is 45 ± 5 minutes.

The variations seen in the outburst subset (including both the rapid-rise and high-state subsets) may well be due to a series of independent events. However, the timescale and amplitude of these events vary in a way that resembles beating between periodic components having different frequencies. Figure 9 shows the reconstruction using two sine waves, with periods of 29.4 and 37.9 minutes. The reconstruction is consistent with the visual impression of beating between components of different frequencies. Assuming that two sine waves are responsible for the oscillations, the 0.1% false alarm level of the periodogram analysis was used to make a more conservative assessment of the periods of the two waves, 27–32 minutes for the highest-amplitude sinusoid and 35–42 minutes for the other sinusoid. While Figure 9 is consistent with the notion that beating between periodic components may be responsible for the unusual oscillatory nature of outburst variations, the duration of the subset is too limited to make this a firm claim.

To further assure that the signals identified by the Scargle periodogram and the CLEAN methods were not seeing-induced effects, the check stars were examined for periodic variations using the same methods. Frequencies identified in the data for PKS 0736+017 would be suspect if those same frequencies were identified in the check star data. The residuals for C2 from the boxcar method are shown in Figure 10. Results from the periodogram analysis for all check stars are summarized in Table 7. The only signal detected for the check stars (boxcar method) was an approximately 20 minute signal. Its identification in the check star data casts suspicion on signals of similar frequency identified in the PKS 0736+017 data. However, examination of Figure 10 suggests that this signal is very likely the result of chance spacings between a few points with large scatter.

TABLE 6

SIGNALS IDENTIFIED IN THE PKS 0736+017 LINEAR-FITS RESIDUALS

SUBSET	SCARGLE PERIODOGRAM RESULTS						CLEAN RESULTS		
	T_1 (minutes)	Prob_1 (%)	T_2 (minutes)	Prob_2 (%)	T_3 (minutes)	Prob_3 (%)	T_1 (minutes)	T_2 (minutes)	T_3 (minutes)
Low	119.2	>99.9	51.1	>99.9	...	...	130.9	50.7	...
Rise	43.8	>99.9	30.0	>99.9	...	...	30.0	40.9	...
High	28.9	>99.9	...	...	...	...	27.8	...	...
Outburst	29.8	>99.9	38.4	>99.9	52.0	99.7	29.4	37.9	22.0
All data	40.1	>99.9	107.4	>99.9	53.7	>99.9	52.2	39.3	105.9

NOTE.—Periods of approximately 20 minutes are obtained from analysis of the check stars (see Table 7) and thus should be considered as suspect.

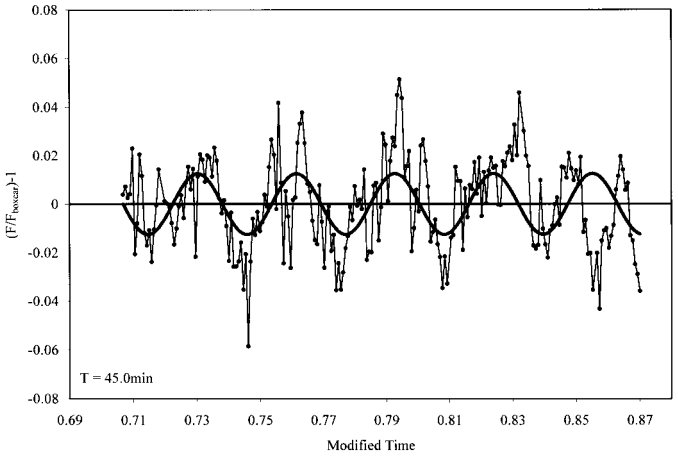

FIG. 8.—Reconstruction of the low-state boxcar residuals using the 45.0 minute sinusoidal variation identified with the CLEAN algorithm.

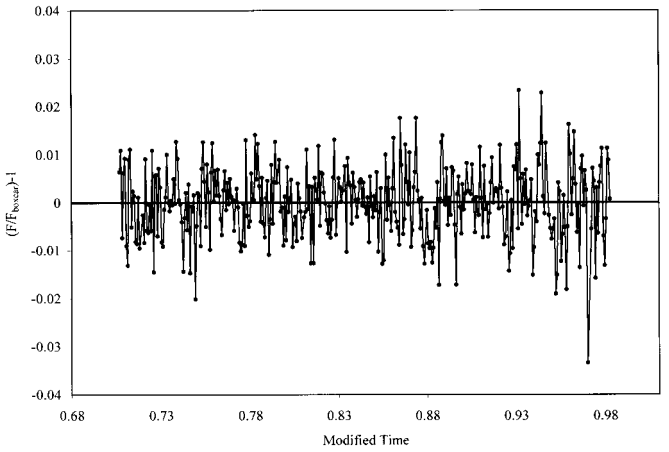

FIG. 10.—Residuals after removal of the boxcar-smoothed data from the data for C2.

3.2. *Color*

Beginning on January 21 observations were made alternately through R and V filters. Prior to computing the colors, the R magnitudes were interpolated to the times of the V observations. Thus, the colors are $V-R_{\rm int}$. The R magnitude was extrapolated to the time of the nearest V observation when it occurred before the first V observation of the night or after the last V observation of the night. The mean colors and the standard deviations in the colors of PKS 0736+017 and the check stars are given in Table 8. The comparison star C1 used for the aperture photometry has magnitudes $V = 15.47 \pm 0.07$ and $R = 14.97 \pm 0.08$ (Smith et al. 1985) and thus has $V-R = 0.40 \pm 0.11$. This is slightly bluer, but fairly close in color, to PKS 0736+017. Figure 11 shows the $V-R_{\rm int}$ color versus time for PKS 0736+017 with the same modified time axis as for Figure 1. (For the check stars see Fig. 12.)

Note that PKS 0736+017 was redder on January 23 (when brighter) than it was on January 21 (when fainter). The more common observation is that sources are "bluer" (have steeper spectra) when brighter (Villata et al. 2002; Clements & Carini 2001; Raiteri et al. 2001; Ghosh et al. 2000; Fan & Lin 1999; Fan et al. 1998; Massaro et al. 1998; Nesci et al. 1998; Speziali & Natali 1998; Webb et al. 1998; Ghisellini et al. 1997; Carini et al. 1992; Gear, Robson, & Brown 1986; Racine 1970) though other behaviors have been noted (Ghosh et al. 2000; Fan & Lin 1999; Maesano et al. 1997; Smith et al. 1992; Kidger et al. 1991; Miller 1981). Perhaps for PKS 0736+017 the observed color variation is related more to the nature of the variation (rising, declining, or quiescent) than to the flux level. Indeed, PKS 0736+017 had approximately the same magnitude at the end of the night on January 21 as it did at the end of the night on January 23, yet its color was distinctly different at the end of the two nights. It was bluer during the flaring event on January 21 $[(V-R_{\rm int})_{\rm ave} = 0.530 \pm 0.014]$ than it was during the subsequent decline on January 23 $[(V-R_{\rm int})_{\rm ave} = 0.596 \pm 0.032]$. In addition, it was slightly redder during the decline on January 23 than during the faint quiescent state on the three subsequent nights $[(V-R_{\rm int})_{\rm ave} = 0.563 \pm 0.031$; average of February 20, March 16, and March 18 data]. Also note that the color remained fairly constant during the January 21 rise, as it did during the January 23 decline. Following Massaro et al. (1998), the change in the spectral index can be computed from the change in color via $\Delta\alpha = 0.4\Delta(V-R)/\log(\lambda_R/\lambda_V)$ or $\Delta\alpha = 5.476\Delta(V-R)$. Thus, from January 21 to January 23 the spectrum

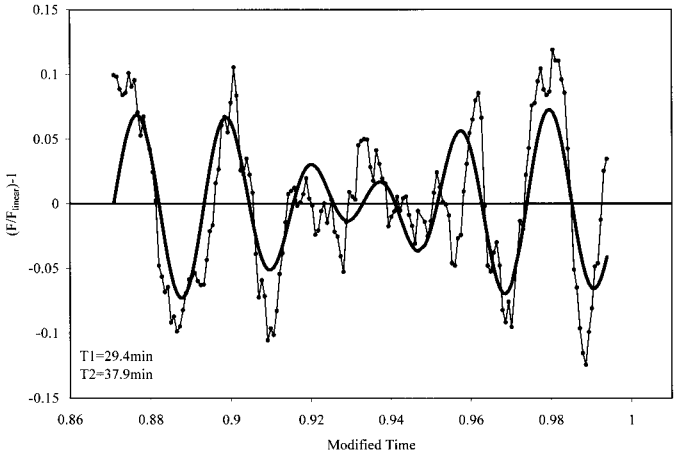

FIG. 9.—Reconstruction of the outburst residuals using the two strongest signals identified using the CLEAN algorithm.

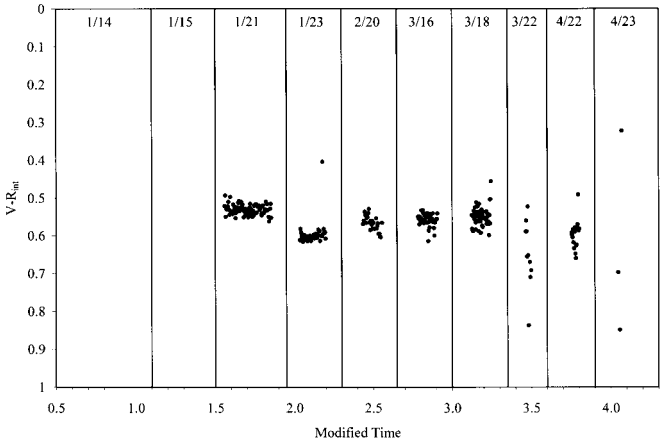

FIG. 11.— $V-R_{\rm int}$ color of PKS 0736+017. The times on the x-axis are modified for display purposes as in Fig. 1.

TABLE 7
SIGNALS IDENTIFIED IN THE CHECK STAR RESIDUALS BY THE PERIODOGRAM ANALYSIS

		BOXCAR RESULTS		LINEAR-FITS RESULTS			
STAR	SUBSET	T_1 (minutes)	Prob_1 (%)	T_1 (minutes)	Prob_1 (%)	T_2 (minutes)	Prob_2 (%)
C2	Low	...	...	250.2	>99.9	100.1	99.7
	Outburst	20.9	96.7	118.1	>99.9	...	...
	All data	21.5	92.8	306.1	>99.9	112.8	>99.9
C3	Low	19.9	91.0	250.2	>99.9	...	...
	Outburst	...	...	126.6	91.0	...	...
	All data	19.8	91.6	238.0	>99.9	109.9	98.1
C4	Low	...	...	65.9	97.1	...	...
	Outburst	...	...	126.6	>99.9	...	...
	All data	...	...	267.8	94.4	109.9	99.7

Only signals with probabilities greater than 90% that random noise is not responsible are listed.

steepened with $\Delta\alpha = 0.361 \pm 0.252$. From January 23 to February 20, the spectrum flattened with $\Delta\alpha = -0.181 \pm 0.345$.

4. DISCUSSION

PKS 0736+017 exhibits numerous variability behaviors during the early 2002 observing run. It exhibited three distinct types of variability behavior on January 14 alone: quasi-periodic variations during its low state, a dramatic flare (or rapid rise), and more complex oscillations during both the rapid-rise and high states.

4.1. *January 14*

4.1.1. *Dramatic Flare*

The impressive flare exhibited by PKS 0736+017 on January 14 is, at 0.6 mag hr^{-1}, among the fastest ever observed for a source. The short timescale and large amplitude suggest a jet phenomenon is at work. A shock in jet with relativistic motion and a small angle to the line of sight is perhaps the most likely explanation for such a dramatic flare. At least consistent with this explanation is the presence of a parsec-scale single-sided jet in radio maps of this source (Bloom et al. 1999; Kellermann et al. 1998). Preliminary results derived from maps on the VLBA 2 cm Survey Web site[2] indicate that all of its three components are superluminal, with apparent speeds of 11.3c (nearest component), 5.2c, and 12.4c (farthest component). The most recent 2 cm VLBA map was made in early 2001 and thus preceded the 2002 January optical flares by a year. Perhaps a future map will show a new component associated with these optical flares emerging from the core.

4.1.2. *Oscillations during the Outburst*

The oscillations which became evident when the source was in its high state have the appearance of beating between signals of different frequencies. Although the data are too limited in duration to unequivocally conclude such beating is present, some support for this qualitative impression is provided by the identification of "periodic" components in the time series analysis of the outburst subset. Such behavior would naturally arise if there were two or more large hot spots at slightly different radii on an accretion disk. However, this would most likely result in smaller fluctuations than observed (0.05 mag or less). (P. Wiita 2002, private communication). Among jet phenomena, a jet precessing near the line of sight or turbulent eddies excited by the

[2] At http://www.cv.nrao.edu/2cmsurvey.

TABLE 8
COLORS OF PKS 0736+017 AND THE CHECK STARS

	PKS 0736+017		C2		C3		C4	
DATE	$(V-R)_{\text{ave}}$	σ_{V-R}	$(V-R)_{\text{ave}}$	σ_{V-R}	$(V-R)_{\text{ave}}$	σ_{V-R}	$(V-R)_{\text{ave}}$	σ_{V-R}
Jan 21	0.530	0.014	0.432	0.010	0.946	0.012	0.467	0.015
Jan 23	0.596	0.032	0.420	0.010	0.930	0.087	0.464	0.018
Feb 20	0.568	0.020	0.430	0.010	0.952	0.015	0.468	0.017
Mar 16	0.559	0.017	0.432	0.015	0.950	0.011	0.467	0.018
Mar 18	0.551	0.026	0.429	0.019	0.946	0.017	0.461	0.020
Mar 20	0.648	0.090	0.466	0.052	0.974	0.050	0.589	0.136
Apr 22	0.598	0.038	0.434	0.033	0.951	0.041	0.472	0.068
Apr 23	0.623	0.271	0.299	0.182	0.865	0.314	0.877	0.378
All	0.563	0.048	0.430	0.029	0.945	0.049	0.475	0.069
Good[a]	0.556	0.032	0.429	0.014	0.944	0.039	0.465	0.018
Good[b]	0.563	0.031	0.431	0.016	0.949	0.015	0.465	0.018

[a] Excludes March 22 and April 23.
[b] Excludes March 22, April 22, and April 23.

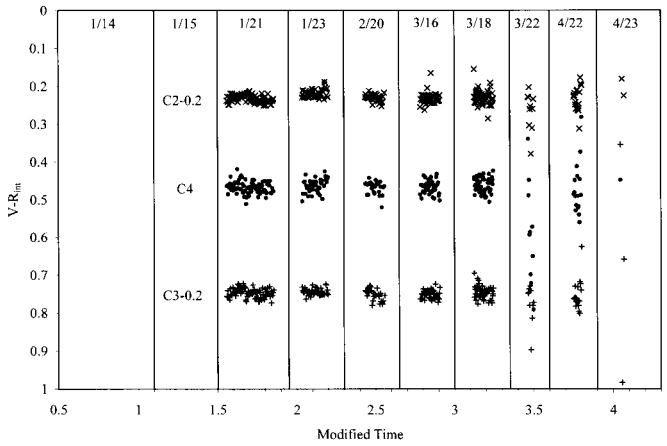

FIG. 12.—$V-R_{\rm int}$ color of the check stars. Note that the colors have been offset for display purposes. Add 0.2 to the colors of C2 and C3 to get their true colors. The times on the x-axis are modified for display purposes as in Fig. 1.

strong shock responsible for the large outburst are other possible explanations for the unusual oscillatory behavior (P. Wiita 2002, private communication).

4.1.3. *Variations during the Low State*

A simple visual inspection of the light curve suggests that PKS 0736+017 exhibits a 45 minute variability timescale during its low state. This impression is supported by the time series analysis, which identified a 45 ± 5 minute periodic signal in the low-state subset. Similar evidence for "periodic" variations with comparable timescales and amplitudes has been reported previously for OJ 287 (39.2 minute variation, Visvanathan & Elliot 1973; 23 minute variation, Carrasco, Dultzin-Hacyan, & Cruz-Gonzalez 1985; 31.4 minute variation, Carini et al. 1992). The explanation for these variations also likely involves a jet phenomenon. However, other explanations are considered. A black hole mass of $(12–22) \times 10^9$ $M_\odot$ was estimated for PKS 0736+017 by McLure et al. (1999) using the Magorrian et al. (1998) black hole–spheroid mass relation. A hot spot orbiting such a black hole would result in variations with observed timescales of months, orders of magnitude longer than those observed here.

Microlensing of a relativistic jet by large planets or small stars in an intervening galaxy as described in Gopal-Krishna & Subramanian (1991) can give rise to the observed timescales. Furthermore, quasi-periodic variations are possible and even expected for the high optical depths that may be needed for large amplifications (Gopal-Krishna & Subramanian 1991). Color variations could be used to help determine if microlensing is a viable explanation. For example, microlensing of a point source is expected to be achromatic. However, observations were made only through the R filter on January 14, so color information is not available to help decipher the source of the variations on this night. The absence of such variations in the observations on subsequent nights argues against microlensing as the source.

4.2. *Observations after January 14*

The evening after its dramatic outburst, PKS 0736+017 had returned to its preflare level. About a week later it was observed to flare again, though more slowly than on January 14. Two days later it was observed to fade even more slowly from its brightest of the observing run. For the remainder of the observing run PKS 0736+017 was observed in a low state. Thus, only the January observing runs captured PKS 0736+017 in an unusually bright state.

M. F. Aller (2002, private communication) reports that PKS 0736+017 was not unusually bright in the radio when observed in late January (after the January optical observations) at 14.5 GHz. H. Teräsranta (2002, private communication) has monitored PKS 0736+017 more regularly at 22 GHz and 37 GHz and reports that in early 2002 PKS 0736+017 underwent its brightest flaring event since 1995. The peak of the event is seen in mid-February. These observations, however, do not have the time resolution to reliably associate the radio and optical flaring events. Past attempts to find correlations between radio and optical events in the long-term light curves of PKS 0736+017 have been unsuccessful, perhaps because of inadequate time sampling (Clements et al. 1995; Tornikoski et al. 1994).

4.3. *Color Variations*

The observation that PKS 0736+017 was redder when it was brighter is unusual. The typical observation that a source is redder when fainter may be due to the relatively redder host galaxy contributing a larger fraction of the total flux when the relatively bluer point source is faint. This was shown to be the likely scenario for BL Lac in 1997 (Clements 2001). Villata et al. (2002) report that during the WEBT BL Lac Campaign 2000, BL Lac became bluer as it brightened even after the galaxy contribution was removed. For the changing contribution of the host galaxy to be responsible for the observed color-brightness relationship reported here for PKS 0736+017, its host galaxy would need to be bluer than the point source. This is not observed. Data from Falomo & Ulrich (2000), Kotilainen, Falomo, & Scarpa (1998), Wright et al. (1998), and Taylor et al. (1996) indicate that the elliptical host galaxy is redder than the nucleus. Furthermore, the source did not vary appreciably in color on January 14 when it brightened by 0.7 mag, nor did it vary appreciably in color on January 21 when it faded by 0.2 mag. Thus, color changes observed for PKS 0736+017 appear to be more related to the nature of the variation, that is whether it was brightening, fading, or in a quiescent state. The color variations of PKS 0736+017 will be further examined in a forthcoming paper (Clements 2004).

5. SUMMARY

Over the course of the early 2002 observing run, PKS 0736+017 exhibited a wide variety of variability behaviors. Most nights it was in a relatively faint state and exhibited only small-scale fluctuations. On three nights, however, it was much brighter and much more variable. The most dramatic event was a very rapid flare that was preceded by quasi-periodic low-amplitude variations. This flare was accompanied by more complex oscillations, which persisted and became most evident once PKS 0736+017 reached its high state. Another dramatic flare was observed about a week later, though this flare was not as rapid. PKS 0736+017 was at its brightest of the observing run a couple of nights later when a still slower steady decline was seen.

PKS 0736+017 also exhibited somewhat unusual color variability. It was redder when at its brightest (January 23). However, the color variations appear to be related more to the nature of the variability than to the source brightness during this observing run.

The authors thank H. Rassoul for his invaluable assistance, as well as P. Wiita, M. Wood, D. Thomas and J. Webb for their helpful comments and suggestions. The authors also greatly appreciate the reviewer's constructive suggestions. This research has made use of the NASA Astrophysics Data System Bibliographic Services, as well as the NASA/IPAC Extragalactic Database. NED is operated by the Jet Propulsion Laboratory, California Institute of Technology, under contract with the National Aeronautics and Space Administration.

REFERENCES

Aller, H. D., Aller, M. F., Latimer, G. E., & Hodge, P. E. 1985, ApJS, 59, 513
Andrew, B. H., McLeod, J. M., Harvey, G. A., & Medd, W. J. 1978, AJ, 83, 863
Antonucci, R., Barvainis, R., & Alloin, D. 1990, ApJ, 353, 416
Bloom, S. D., Marscher, A. P., Moore, E. M., Gear, W., Teräsranta, H., Valtaoja, E., Aller, H. D., & Aller, M. F. 1999, ApJS, 122, 1
Carini, M. T., Miller, H. R., Noble, J. C., & Goodrich, B. D. 1992, AJ, 104, 15
Carrasco, L., Dultzin-Hacyan, D., & Cruz-Gonzalez, I. 1985, Nature, 314, 146
Cellone, S. A., Romero, G. E., & Combi, J. A. 2000, AJ, 119, 1534
Clements, S. D. 2001, BAAS, 199, No. 9811
———. 2004, ApJ, in preparation
Clements, S. D., & Carini, M. T. 2001, AJ, 121, 90
Clements, S. D., Smith, A. G., Aller, H. D., & Aller, M. F. 1995, AJ, 110, 529
Deeming, T. J. 1975, Ap&SS, 36, 137
Falomo, R., & Ulrich, M.-H. 2000, A&A, 357, 91
Fan, J. H., & Lin, R. G. 1999, ApJS, 121, 131
Fan, J. H., Xie, G. Z., Pecontal, E., Pecontal, A., & Copin, Y. 1998, ApJ, 507, 173
Fossati, G., Maraschi, L., Celotti, A., Comastri, A., & Ghisellini, G. 1998, MNRAS, 299, 433
Gear, W. K., Robson, E. I., & Brown, M. J. 1986, Nature, 324, 546
Ghisellini, G., et al. 1997, A&A, 327, 61
Ghosh, K. K., Ramsey, B. D., Sadun, A. C., & Soundararajaperumal, S. 2000, ApJS, 127, 11
Gopal-Krishna & Subramanian, K. 1991, Nature, 349, 766
Gopal-Krishna, Sagar, R., & Wiita, R. J. 1993, MNRAS, 262, 963
Gower, A. C., & Hutchings, J. B. 1984, AJ, 89, 1658
Hogbom, J. A. 1974, A&AS, 15, 417
Horne, J. H., & Baliunas, S. L. 1986, ApJ, 302, 757
Impey, C. D., & Neugebauer, G. 1988, AJ, 95, 307
Jang, M., & Miller, H. R 1995, ApJ, 452, 582
———. 1997, AJ, 114, 565
Kellermann, K. I., Sramek, R. A., Schmidt, M., Green, R. F., & Shaffer, D. B. 1994, AJ, 108, 1163
Kellermann, K. I., Vermeulen, R. C., Zensus, J. A., & Cohen, M. H. 1998, AJ, 115, 1295
Kidger, M. R., Takalo, L. O., Valtaoja, E., de Diego, J. A., & Sillanpää, A. 1991, A&A, 252, 538
Kotilainen, J. K., Falomo, R., & Scarpa, R. 1998, A&A, 332, 503
Lynds, C. R. 1967, ApJ, 147, L837
Maesano, M., Montagni, F., Massaro, E., & Nesci, R. 1997, A&AS, 122, 267
Magorrian, J., et al. 1998, AJ, 115, 2285
Massaro, E., Nesci, R., Maesano, M., Montagni, F., & D'Alessio, F. 1998, MNRAS, 299, 47
Matthews, T. A., & Sandage, A. R. 1963, ApJ, 138, 30
McLure, R. J., Kukula, M. J., Dunlop, J. S., Baum, S. A., O'Dea, C. P., & Hughes, D. H. 1999, MNRAS, 308, 377
Medd, W. F., Andrew, B. H., Harvey, G. A., & Locke, F. L. 1973, MNRAS, 163, 437
Miller, H. R. 1981, ApJ, 244, 426
Miller, H. R., Carini, M. T., & Goodrich, B. D. 1989, Nature, 337, 627
Miller, R., Rawlings, S., & Saunders, R. 1993, MNRAS, 263, 425
Nesci, R., Maesano, M., Massaro, E., Montagni, F., Tosti, G., & Fiorucci, M. 1998, A&A, 332, L1
Pica, A. J., Smith, A. G., Webb, J. R., Leacock, J. L., Clements, S., & Gombola, P. P 1988, AJ, 96, 1215
Pollock, J. T. 1999, BAAS, 195, No. 1505
Racine, R. 1970, ApJ, 159, L99
Raiteri, C. M., et al. 2001, A&A, 377, 396
Roberts, D. H., Lehár, J., & Dreher, J. W. 1987, AJ, 93, 968
Romney, J., et al. 1984, A&A, 135, 289
Sagar, R., Gopal-Krishna, & Wiita, P. J. 1996, MNRAS, 281, 1267
Scargle, J. D. 1982, ApJ, 263, 835
Smith, P. S., Balonek, T. J., Elston, R., & Schmidt, G. D. 1985, AJ, 90, 1184
Smith, P. S., Hall, P. B., Allen, R. G., & Sitko, M. L. 1992, ApJ, 400, 115
Speziali, R., & Natali, G. 1998, A&A, 339, 382
Tadhunter, C. N., Morganti, R., de Serego Alighieri, S., Fosbury, R. A. E., & Danziger, I. J. 1993, MNRAS, 263, 999
Taylor, G. L., Dunlop, J. S., Hughes, D. S., & Robson, E. I. 1996, MNRAS, 283, 930
Teräsranta, H., et al. 1998, A&AS, 132, 305
Tornikoski, M., Valtaoja, E., Teräsranta, H., Smith, A. G., Nair, A. D., Clements, S. D., & Leacock, R. J. 1994, A&A, 289, 673
Véron-Cetty, M.-P., & Véron, P. 2001, A&A, 374, 92
Villata, M., et al. 2002, A&A, 390, 407
Visvanathan, N., & Elliot, J. L. 1973, ApJ, 179, 721
Wagner, S. J., & Witzel, A. 1995, ARA&A, 33, 163
Webb, J. R., et al. 1998, AJ, 115, 2244
Wiita, P. J. 1993, in Accretion and Jets in Astrophysics, ed. Li Qibin, Yang Lantian, Xie Guangzhong, & Yang Pibo (Wuhan: Huazhong Normal Univ. Press), 1
Wilkat, V. L., Webb, J. R., Clements, S. D., & Pollock, J. T. 2002, BAAS, 201, No. 4801
Wright, S. C., McHardy, I. M., & Abraham, R. G. 1998, MNRAS, 295, 799